

## Article

# New Functions of Low-Molecular-Weight Hyaluronic Acid on Epidermis Filaggrin Production and Degradation

Moe Hashimoto <sup>1</sup> and Kazuhisa Maeda <sup>1,2,\*</sup> 

<sup>1</sup> Bionics Program, Tokyo University of Technology Graduate School, 1404-1 Katakuramachi, Hachioji City 192-0982, Tokyo, Japan; g111704733@edu.teu.ac.jp

<sup>2</sup> School of Bioscience and Biotechnology, Tokyo University of Technology, 1404-1 Katakuramachi, Hachioji City 192-0982, Tokyo, Japan

\* Correspondence: kmaeda@stf.teu.ac.jp; Tel.: +81-42-588-7752

**Abstract:** Hyaluronic acid (HA) is a high-molecular-weight polysaccharide with high moisturizing power. It is composed of repeating disaccharides of N-acetyl-D-glucosamine and D-glucuronic acid. Low-molecular-weight hyaluronan (LMHA) is obtained by changing the molecular weight or modifying the functional groups of HA and is commonly used together with HA in cosmetics. The objective of this study was to determine whether LMHA promotes the synthesis of filaggrin (FLG). We also investigated whether LMHA activates FLG-degrading enzymes. Three-dimensional (3D) models of the human epidermis were cultured with LMHA. Real-time PCR was used to quantify the mRNA levels of profilaggrin (proFLG), involucrin (IVL), and FLG-degrading enzymes. FLG protein levels were measured by fluorescent antibody staining and Western blotting. The mRNA was quantified using a 3D epidermis model, and it was observed that the mRNA levels of proFLG, IVL, caspase-14 (CASP14), and bleomycin hydrolase were increased by the application of LMHA. Immunofluorescence results showed an increase in FLG proteins, and results from experiments using 3D epidermis models showed that LMHA increased the activity of CASP14. This suggests that the topical application of LMHA would result in an increase in natural moisturizing factor and promote moisturization of the stratum corneum.

**Keywords:** hyaluronic acid; filaggrin; caspase-14; bleomycin hydrolase; moisture; skincare



**Citation:** Hashimoto, M.; Maeda, K. New Functions of Low-Molecular-Weight Hyaluronic Acid on Epidermis Filaggrin Production and Degradation. *Cosmetics* **2021**, *8*, 118. <https://doi.org/10.3390/cosmetics8040118>

Academic Editor:  
Pierfrancesco Morganti

Received: 6 November 2021  
Accepted: 13 December 2021  
Published: 16 December 2021

**Publisher's Note:** MDPI stays neutral with regard to jurisdictional claims in published maps and institutional affiliations.



**Copyright:** © 2021 by the authors. Licensee MDPI, Basel, Switzerland. This article is an open access article distributed under the terms and conditions of the Creative Commons Attribution (CC BY) license (<https://creativecommons.org/licenses/by/4.0/>).

## 1. Introduction

The skin has an important barrier function that prevents stimulation from the outside world and moisture evaporation from inside the body. The main factors that maintain this barrier function are the cornified cell envelope (CE) of stratum corneum cells, natural moisturizing factor (NMF) produced by the breakdown of proteins such as filaggrin (FLG), and intercellular lipids of the stratum corneum. The main component of the CE of stratum corneum cells is a protein called involucrin (IVL). NMF is known to be essential for skin moisturization, and amino acids and their derivatives are the main components of NMF. NMF is derived from FLG and is closely related to skin hydration. FLG is a protein involved in differentiation that aggregates keratin fibers and the skeletal protein of the stratum corneum and strengthens the internal structure of the stratum corneum [1]. ProFLG, which consists of 10 to 12 FLG units, is stored in the stratum granulosum and, upon keratinization, it is excised by kallikrein-5 (KLK5) and other proteins to become individual FLGs [2]. When FLG is dephosphorylated, it polymerizes with keratin to form the internal structure of stratum corneum cells called the keratin pattern. The FLG then becomes susceptible to deimination [3] and is degraded by proteolytic enzymes such as calpain-1 (CAPN1), caspase-14 (CASP14), and bleomycin hydrolase (BLMH) to form NMF [4]. The degradation of proFLG to NMF is shown in Figure 1. Several pathways such as the N-terminus of FLG are said to be involved in DNA degradation during keratinocyte terminal differentiation [5].

Recently, it has been reported that abnormalities in the FLG gene are a major factor in the pathogenesis of ichthyosis vulgaris and atopic dermatitis (AD) [6,7].

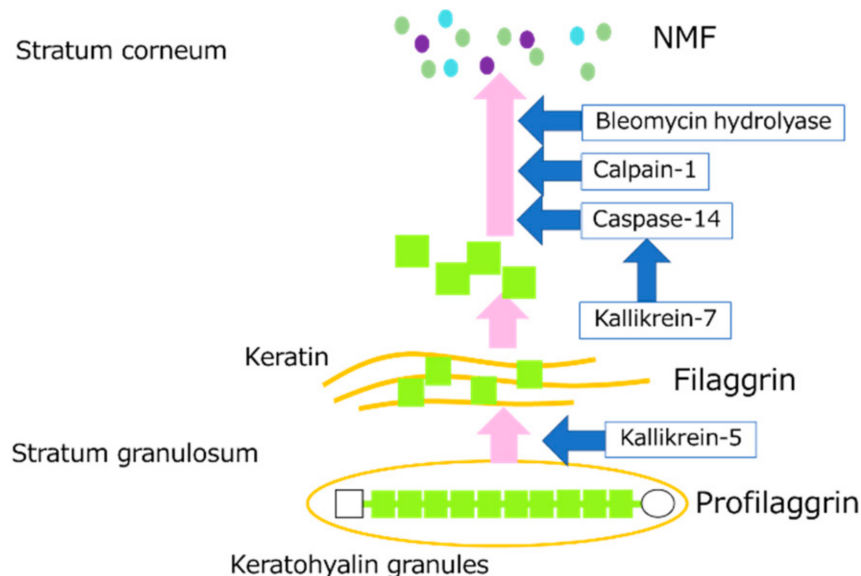


**Figure 1.** Diagram showing the degradation pathway of proFLG to NMF in the stratum granulosum and stratum corneum.

CASP14, CAPN1, and BLMH are FLG-degrading enzymes. CASP14 is a cysteine-aspartic acid protease. Although most CASPs are part of signaling pathways that cause cellular apoptosis, CASP14 is not involved in such pathways [8]. Lower levels of CASP14 are often identified in patients with atopic dermatitis and psoriasis [9]. CAPNs are cysteine proteases, and are classified into two groups,  $\mu$ -calpain and m-calpain, depending on their calcium ion sensitivity. The  $\mu$ -calpain is highly sensitive to calcium [10]. CAPN1, one of the  $\mu$ -calpains, is activated by calcium ions. BLMH is universally present in all tissue, with the highest concentrations found in the skin. Patients with atopic dermatitis have been reported to have decreased levels of skin BLMH [11].

Kallikrein (KLK) is a type of serine protease. Fifteen types of tissue KLK have been reported so far in humans, 12 of which are expressed in the epidermis [12]. KLK5 and KLK7 are particularly highly expressed in the skin [13,14]. KLK5 is a trypsin-like serine protease that cleaves the C-terminus of arginine and lysine, while KLK7 is a chymotrypsin-like serine protease that cleaves the C-terminus of tyrosine and phenylalanine [15]. They act as substrates for the cell adhesion molecules desmoglein, desmocollin, and corneodesmosin and are involved in stratum corneum exfoliation [16]. KLK5 is responsible for cleaving proFLG into FLG monomers [2], while KLK7 plays an important role in the activation pathway of CASP14, a FLG-degrading enzyme [8]. Recently, KLK8 and KLK14 have also been found to be involved in stratum corneum exfoliation [17].

Hyaluronic acid (HA) is a high-molecular-weight polysaccharide composed of repeating disaccharides of N-acetyl-D-glucosamine and D-glucuronic acid. HA is a component of the extracellular matrix and is found in the dermis of the skin and the lens of the eye. In the skin, it is involved in differentiation and epidermal responses [18]. Some studies indicate that aging and exogenous stimuli such as solar UV rays, smoking, and air pollutants decrease the levels of HA in the skin. In recent years, HA has been widely used in healthy foods and moisturizing skincare products [19]. Low-molecular-weight hyaluronan (LMHA) is obtained by changing the molecular weight or modifying the functional groups of HA. In contrast to the stratum corneum impermeability of high-molecular-weight HA (1000–1400 kDa), the LMHA (20–300 kDa) has been reported to pass through the stratum corneum by Raman spectroscopy [20]. The LMHA of approximately 50 kDa influences the expression of various genes including those contributing to keratinocyte differentiation



and formation of intercellular tight junction complexes without showing proinflammatory activity [21]. It has been reported that 0.5% LMHA (of 20–50 kDa) promotes ceramide synthesis by rearranging the lipidome in cultured human dermal fibroblasts [22]. On the other hand, the average molecular weight of LMHA used in this study is less than 10 kDa. This also has moisturizing effects and is also widely used in skincare products.

The objective of this study was to investigate whether the topical application of LMHA with an average molecular weight of less than 10 kDa, to three-dimensional reconstructions of the human epidermis (3D epidermis models) could promote the synthesis of FLG. In addition, the contribution of FLG-degrading enzymes in increasing NMF was assessed by measuring the amount of mRNA of these enzymes and other associated factors.

## 2. Materials and Methods

### 2.1. Quantification of mRNA in 3D Epidermis Model with Topically Applied LMHA

#### 2.1.1. The 3D Epidermis Model

The 3D epidermis models (LabCyte EPI-MODEL) were purchased from Japan Tissue Engineering Co. Ltd. (Aichi, Japan). The aluminum-wrapped 3D epidermis models in the cup fixed to agar plate transported at room temperature were transferred to Falcon 24 well tissue culture plates containing 0.5 mL of dedicated medium and used for experiments starting the next day. The LabCyte EPI-MODEL is a human 3D cultured epidermis model in which normal human epidermal cells are cultured in layers and can be used to evaluate the toxicity and irritation of test substances. Because the cells retain metabolic activity, the model can be used for dermatological research such as measuring the production of inflammatory factors and cell growth factors, and for pharmacological research of various drugs [23,24].

#### 2.1.2. Application of LMHA to the 3D Epidermis Model

Ten milligrams of LMHA (Kewpie Corporation, Tokyo, Japan) were weighed and dissolved in 2 mL of ultrapure water to prepare an aqueous solution of 5 mg/mL LMHA. Ultrapure water was used alone as a control. The aqueous solution and the control water were sterilized using a sterile filter. Twenty microliters of the prepared aqueous solution were topically applied to the 3D epidermis models ( $n = 3$ ), and then incubated at 37 °C for 2 days.

#### 2.1.3. RNA Extraction from the 3D Epidermis Model

One hundred microliters of mercaptoethanol (Fujifilm, Wako Pure Chemical Corporation, Osaka, Japan) was added to 10 mL of buffer RLT from the RNeasy<sup>®</sup> Protect Mini Kit (Qiagen N.V., Venlo, The Netherlands), and 350  $\mu$ L was added to each microtube. The epidermis models were removed from a cup with tweezers and added to the tubes. The epidermis model was reduced to small pieces by pipetting. A column was set in each tube and the sample was added to the column. The tubes were then centrifuged at 11,000 rpm for 2 min, the columns were removed, and 350  $\mu$ L of 70% ethanol was added to each. The tubes were centrifuged again at 11,000 rpm for 15 s, and then 500  $\mu$ L of buffer RPE was added to each. After two more minutes in the centrifuge at 11,000 rpm, the columns were transferred to new tubes. Thirty microliters of RNase-free water were added to each column and centrifuged at 11,000 rpm for 1 min, and then 30  $\mu$ L of RNase-free water was added and further centrifuged at 11,000 rpm for another minute. The tubes were covered with lids and stored in a freezer at  $-30$  °C.

#### 2.1.4. mRNA Quantification by Real-Time PCR Using 3D Epidermis Model

The One-Step SYBR<sup>®</sup> PrimeScript<sup>™</sup> RT-PCR kit II (Takarabio Inc., Shiga, Japan) was used to prepare the reaction solution as per the manufacturer's instructions, and 16.4  $\mu$ L of the solution was added to a 96-well plate for the PCR. The composition of the reaction solution was as follows: 2x One-Step SYBR RT-PR Buffer 4 (10  $\mu$ L), PrimerScript One-Step Enzyme Mix 2 (0.8  $\mu$ L), ROX Reference Dye (0.4  $\mu$ L), and RNase-free dH<sub>2</sub>O (5.2  $\mu$ L).

Primers for proFLG, IVL, CASP14, CAPN1, BLMH, KLK5, KLK7, and the housekeeping genes,  $\beta$ -actin (Qiagen N.V.) were used. For each sample, 1.6  $\mu$ L of primer was placed in a container. Next, 2  $\mu$ L of the sample was added to each (total volume 20  $\mu$ L). After confirming that there were no air bubbles at the bottom, the lids were put on and the samples were prepared for real-time PCR. The temperature conditions were as follows: Stage 1: 42 °C/5 min, Stage 2: 95 °C/10 s, Stage3: 95 °C/5 s, Stage 4: 95 °C/15 s, Stage 5: 95 °C/15 s, 60 °C/1 min, and 95 °C/15 s. After measurement, the data was analyzed by the  $\Delta\Delta$ Ct method in a real-time PCR device (ABI PRISM 7900HT, Applied Biosystems Co., Ltd., Waltham, MA, USA). The experiment was performed three times.

## 2.2. Immunohistochemical Staining of the 3D Epidermis Models

### 2.2.1. Culture of the 3D Epidermis Models

Twenty microliters each of the 5 mg/mL aqueous solution of filter sterilized LMHA and ultrapure water (control) were topically applied to the 3D epidermis models ( $n = 3$ ) and incubated at 37 °C for 3 days.

### 2.2.2. Tissue Section Preparation

Embedding agent for frozen tissue section production (Tissue-Tek<sup>®</sup> O.C.T. Compound; Sakura Finetek Japan Co., Ltd., Tokyo, Japan) was added to the embedding dish. The 3D epidermis models were removed with a Derma Punch (Maruho Co., Ltd. Osaka, Japan) and submerged vertically in the embedding dish using tweezers. The embedding dish was added to plastic containers on dry ice and frozen. Once completely frozen, they were thinly sliced to 10  $\mu$ m using a Cryostat (Leica Biosystems Nussloch GmbH, Wetzlar, Germany) and collected on glass slides.

### 2.2.3. FLG Immunofluorescence

The tissues placed on glass slides (as described in Section 2.2.2) were removed from the freezer and a large border using a Super PAP Pen (Daido Sangyo Co., Ltd., Tokyo, Japan) was placed around each tissue. After three washes with PBS, 10% goat serum PBS solution was added to each sample and left for 30 min. After two additional washes with PBS, the first antibody (human anti-FLG rabbit polyclonal antibody (Atlas Antibodies AB, Bromma, Sweden) in PBS solution) was added and incubated for 1 h. After washing with PBS, the second antibody (Alexa Flour 488 goat anti-rabbit IgG (H+L) (Thermo Fisher Scientific Inc., Waltham, MA, USA) in PBS solution) was added and allowed to stand for 1 h. After washing, nuclear staining was performed with DAPI (1000-fold dilution; Dojindo Laboratories, Kumamoto, Japan) for 5 min. Each sample was washed with pure water and drained. A few drops of inclusion agent were added to each of the containers, which were then covered with glass. The samples were observed and photographed under an inverted fluorescence microscope (IX70, Olympus Corporation, Tokyo, Japan). The FLG staining was taken with WIB and nuclear staining with WU. The experiment was performed three tissue sections.

## 2.3. Staining for CASP14 Activity in the 3D Epidermis Models

The substrate (Ac-Trp-Glu-His-Asp-pNA) was dissolved in DMSO to 10 mmol/L, and 2  $\mu$ L of this was mixed with 86  $\mu$ L of PBS. FastBlue was dissolved in 75% N, N-dimethylformamide to 50 mg/mL and further adjusted to 5.5 mg/mL with PBS. Eighty-eight microliters of substrate solution and 22  $\mu$ L of FastBlue solution were mixed (concentration of substrate: 0.18 mmol/L, concentration of FastBlue: 1.1  $\mu$ g/ $\mu$ L). The tissues were removed from the freezer, trimmed, and the substrate solution was added to cover each tissue sample. These were then covered with glass. Images were taken using an inverted confocal laser scanning microscope (FV3000, Olympus Corporation) with an excitation wavelength of 359 nm and a fluorescence wavelength of 461 nm. The experiment was performed three tissue sections.

#### 2.4. Staining for CAPN1 Activity in the 3D Epidermis Models

Two microliters of the substrate (Suc-Leu-Leu-Val-Tyr-pNA) was dissolved in DMSO to 10 mmol/L. FastBlue was dissolved in 75% N, N-dimethylformamide to 50 mg/mL and further adjusted to 5.5 mg/mL with PBS plus 100  $\mu$ mol/L CaCl<sub>2</sub>. Eighty-eight microliters of substrate solution and 22  $\mu$ L of FastBlue solution were then mixed (concentration of substrate: 0.18 mmol/L, concentration of FastBlue: 1.1  $\mu$ g/ $\mu$ L). The tissue samples were removed from the freezer, trimmed, and the substrate solution was added to cover the tissue. Images were taken using an inverted confocal laser scanning microscope (FV3000) with an excitation wavelength of 359 nm and a fluorescence wavelength of 461 nm. The experiment was performed three tissue sections.

#### 2.5. Measurement of BLMH Activity Using Human Epidermal Keratinocytes

Human immortal epidermal keratinocytes (HaCaT; Cell Lines Service GmbH Eppelheim, Germany) were cultured in DMEM containing 10% FBS. Then, 10 mL of trypsin was added, and the cells were removed by incubating at 37 °C for 30 min. This solution and 10 mL of medium were then added to a tube and centrifuged for 5 min. The supernatant was removed, and 10 mL of medium was added and mixed by pipetting. The number of cells was measured with a cell counter and then 350,000 cells were seeded in 100 mm dishes to which 100  $\mu$ L of control (sterile water), 5 mg/mL HA, and 5 mg/mL LMHA were added ( $n = 3$ ). The cells were incubated at 37 °C for 2 days. The medium was removed, and the surface was washed with PBS. One milliliter of extraction buffer (PBS solution of 1% sodium deoxycholate and 1% triton X-100) was added, and the cells were scraped up with a cell scraper, added to an Eppendorf tube, and mixed by vortexing the tube.

For BLMH activity, L-citrulline 7-amido-4-methylcoumarin hydrobromide (Santa Cruz Biotechnology, Inc., Dallas, TX, USA) was dissolved in PBS to prepare a 1 mM substrate solution. To a 96-well plate, 60  $\mu$ L of cell extracts and 40  $\mu$ L of the prepared L-citrulline 7-amido-4-methylcoumarin hydrobromide solution was added to the wells. Next, a fluorescence microplate reader (Multi-Detection Microplate Powersan HT; BioTek, Winooski, VT, USA) was used to measure the fluorescence intensity at a wavelength of 360/460 nm of the solution for activity measurement. The change in fluorescence intensity (0 to 120 min) was calculated. For protein quantification, 10  $\mu$ L of cell extract was used. The Pierce™ BCA protein assay kit (Thermo Fisher Scientific Inc.) was used for protein level measurement. The absorbance was measured at 562 nm, the reaction was carried out at 37 °C, and the fluorescence intensity was measured after 60 min. A calibration curve for protein was prepared and the amount of protein in each sample was determined. The changes in fluorescence intensity and amount of protein were calculated, and the enzyme activity was calculated. The experiment was performed three times.

#### 2.6. Hyaluronan Staining of the 3D Epidermis Models

A border was placed around the tissue section of the 3D epidermis models (as described in Section 2.2.2). The tissue sections were fixed with 4% paraformaldehyde at 4 °C for 10 min and washed with PBS. The tissue sections were then immersed in 3% acetic acid for 3 min, in Alcian blue solution (pH 2.5) for 50 min, and in 3% acetic acid for 3 min. Then, they were rinsed with running water and distilled water. The inclusion agent was added, covered with glass, and observed under a microscope. The experiment was performed three tissue sections.

Alcian blue is a basic dye belonging to the phthalocyanine family. Its ions bind to the carboxyl and sulfate groups of acidic mucopolysaccharides. At low pH levels (pH = 1.0 or lower), only the sulfate group binds to the dye, so mucopolysaccharides containing sulfate groups are selectively stained depending on the pH value.

#### 2.7. Western Blotting of the 3D Epidermis Models

Forty microliters of sterile water (control), 2.5 mg/mL and 5 mg/mL of HA, and 1.25 mg/mL, 2.5 mg/mL, and 5 mg/mL LMHA were added to the 3D epidermis models

and incubated at 37 °C for 2 days. After incubation, holes were made in the 3D epidermis models with the Derma Punch, and the membrane and epidermis model were added to an Eppendorf tube. To this, 300 µL of SDS sample buffer was added, mixed by vortexing, and stored in a freezer. Later, the samples were heated at 95 °C for 5 min and centrifuged. Ten microliters of molecular weight marker were used (left lane, no. 1) on an SDS-PAGE gel (two gels were used). On the gels, lane no. 3 was control (solvent), lanes 4 and 5 were topically applied with HA, and lanes 9 to 11 were topically applied with LWHA. Electrophoresis was performed at 54 mA (about 50 V) for 2 h. The membrane was dipped in methanol for 10 s and then immersed in transfer buffer along with filter paper and a pad for at least 15 min. After electrophoresis was completed, the excess gel was cut off and added to the transfer buffer. From the negative electrode core, in the following order, stacks were made of the pads, filter paper, gel, membrane, filter paper, pads, filter paper, gel, membrane, filter paper, and pads. These were fixed in the electrophoresis layer. They were then washed three times for 5 min, and then incubated in a blocking buffer for 1 h. They were then washed three times for 5 min, this time with Tris-buffered saline with 0.05% Tween 20 (TBS-T). Primary antibodies used were as follows: anti-FLG antibody (rabbit) diluted 200×, human anti-IVL mouse antibody (Sigma-Aldrich Corp., St. Louis, MO, USA) diluted 1000×, human anti-loricrin rabbit antibody (Proteintech Group, Inc., Rosemont, IL, USA) diluted 1000×, human anti-transglutaminase 1 (TGM1) rabbit antibody (Proteintech Group, Inc.) diluted 1000×, and human anti-beta-actin mouse antibody (Proteintech Group, Inc.) diluted 10,000× in TBS. After three washes with TBS-T for 5 min, each antibody was diluted 5000 times with the appropriate secondary antibody and washed six times (1 h) with TBS-T. Each antibody was immersed in a 1:1 mixture of A and B of Amersham ECL select Western blotting detection reagent (GE Healthcare, Chicago, IL, USA) and the images were recorded. The photographs were analyzed using ImageJ software.

### 2.8. Statistical Analysis

Numerical data were recorded in Microsoft Excel, and the means and standard deviations were calculated. Two-tailed t-tests were performed, with  $p < 0.05$  considered statistically significant (Sections 2.1 and 2.5).

## 3. Results

### 3.1. mRNA Quantification of proFLG, IVL, CASP14, CAPN1, BLMH, KLK5, and KLK7 in the 3D Epidermis Models

Three-dimensional epidermis models were topically applied with 5 mg/mL LMHA solution and cultured for 2 days. mRNA was extracted and real-time PCR was performed. The primers used were IVL as a differentiation marker; proFLG; CASP14, CAPN1, and BLMH as FLG-degradation enzymes; KLK5 as a trypsin-like enzyme; and KLK7 as a CAPS14-activating enzyme.

The results of the quantitative analysis of the mRNA are shown in Figure 2. All results were compared with  $\beta$ -actin. FLG is responsible for aggregating keratin proteins, the skeletal proteins of the stratum corneum. Subsequently, FLG is degraded into NMF, which is essential for moisturization. The mRNA levels of proFLG, IVL, CASP14, and BLMH were significantly higher in the LMHA-applied 3D epidermis model than in the solvent (control)-applied 3D epidermis model. The level of CAPN1 was not significantly different between the LMHA-applied 3D epidermis model and the solvent (control)-applied 3D epidermis model. The mRNA level of BLMH enzyme, which is also an enzyme that degrades FLG, was significantly higher in the LMHA-applied epidermis model than in the solvent (control)-applied 3D epidermis model. KLK7 plays an important role in the formation of intermediates during the activation of CASP14. KLK5 and KLK7 are thought to act as substrates for the cell adhesion molecules desmoglein, desmocollin, and corneodesmosin, which promote stratum corneum detachment. The level of mRNA of KLK7 was significantly higher in the LMHA-applied 3D epidermis model than in the solvent (control)-applied 3D epidermis model. The level of CAPN1 was not significantly

different between the LMHA-applied 3D epidermis model and the solvent (control)-applied 3D epidermis model. The mRNA level of BLMH enzyme, which is also an enzyme that degrades FLG, was significantly higher in the LMHA-applied epidermis than in the solvent (control)-applied 3D epidermis model.

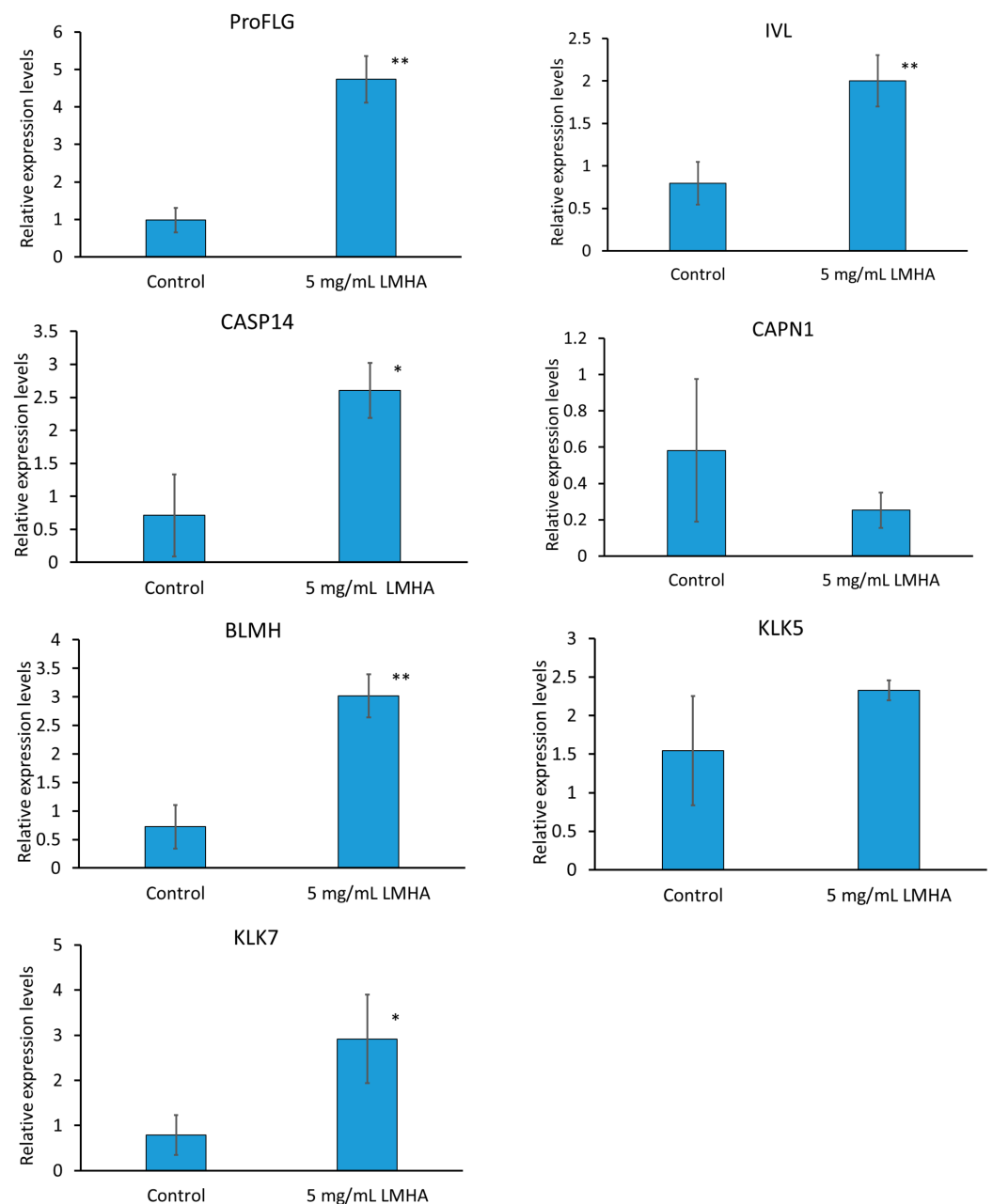


**Figure 2.** Effects of topical application of LMHA on the mRNA levels of proFLG, IVL, CAPN1, CASP14, BLMH, KLK 5, and KLK7 in the 3D epidermis models.  $n = 3$ , mean  $\pm$  standard deviation, \*  $p < 0.05$  vs. control. \*\*  $p < 0.01$  vs. control.

### 3.2. Immunohistochemical Staining of FLG in the 3D Epidermis Models

To examine whether the immunoreactivity of FLG was increased in LMHA with higher proFLG mRNA levels, fluorescence antibody against FLG was used. The results are shown below as bright field, nuclear staining, and FLG staining. The fluorescence intensity of immunoreactive FLG (bottom of Figure 3) was greater near the stratum corneum in the 3D epidermis model with topically applied LMHA compared to a model with topically



applied solvent (control). In addition, nuclei were observed near the stratum corneum in the control epidermis models.

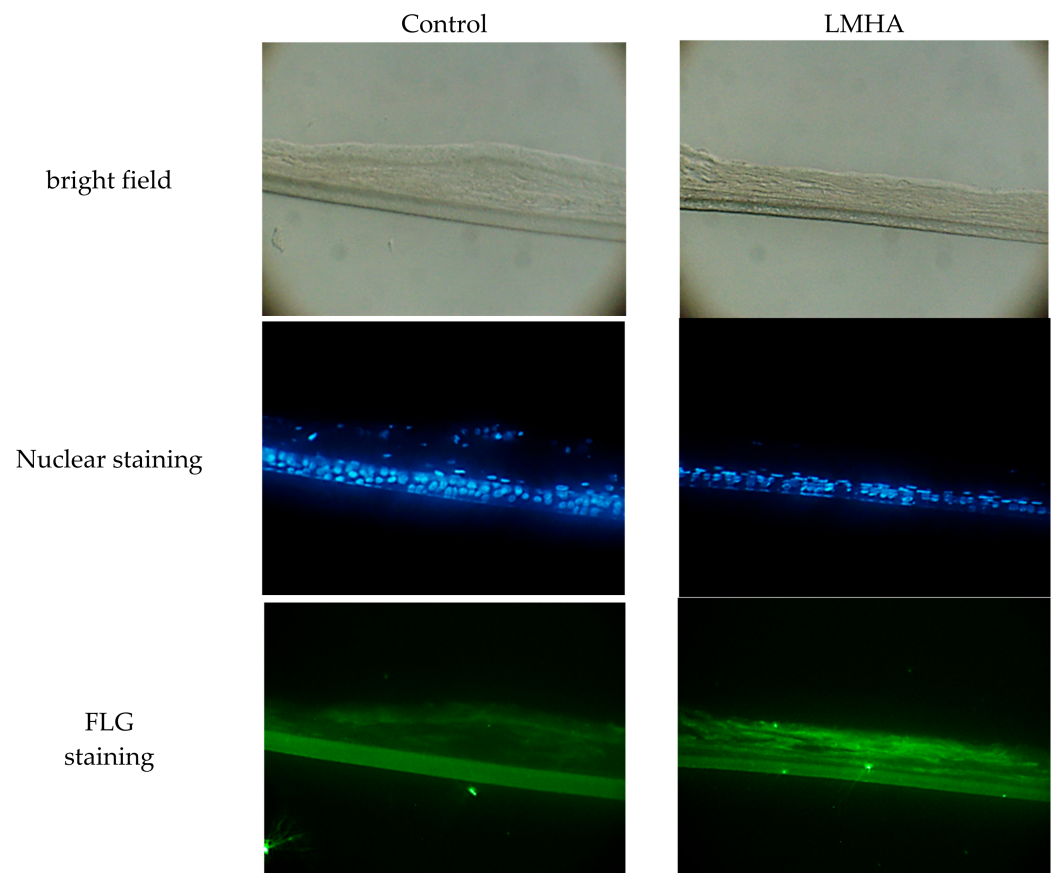


**Figure 3.** Immunoreactive FLG in 3D epidermis models with topically applied either LMHA or solvent (control).

### 3.3. Staining for CASP14 Activity in the 3D Epidermis Models

Staining for CASP14 was performed using Ac-WEHD-pNA (Ac-Trp-Glu-His-Asp-pNA) as a substrate in tissue sections applied with LMHA or solvent (control) in which an increase in immunoreactive FLG was observed. FastBlue was used as the staining reagent, and the images were observed at 359/461 nm using an inverted confocal laser scanning microscope. Bright field and fluorescence images were taken at 100× magnification and the areas where fluorescence was observed were magnified. Higher fluorescence intensity was observed in the stratum corneum to stratum granulosum in the 3D epidermis model applied with LMHA compared to the control (Figure 4).

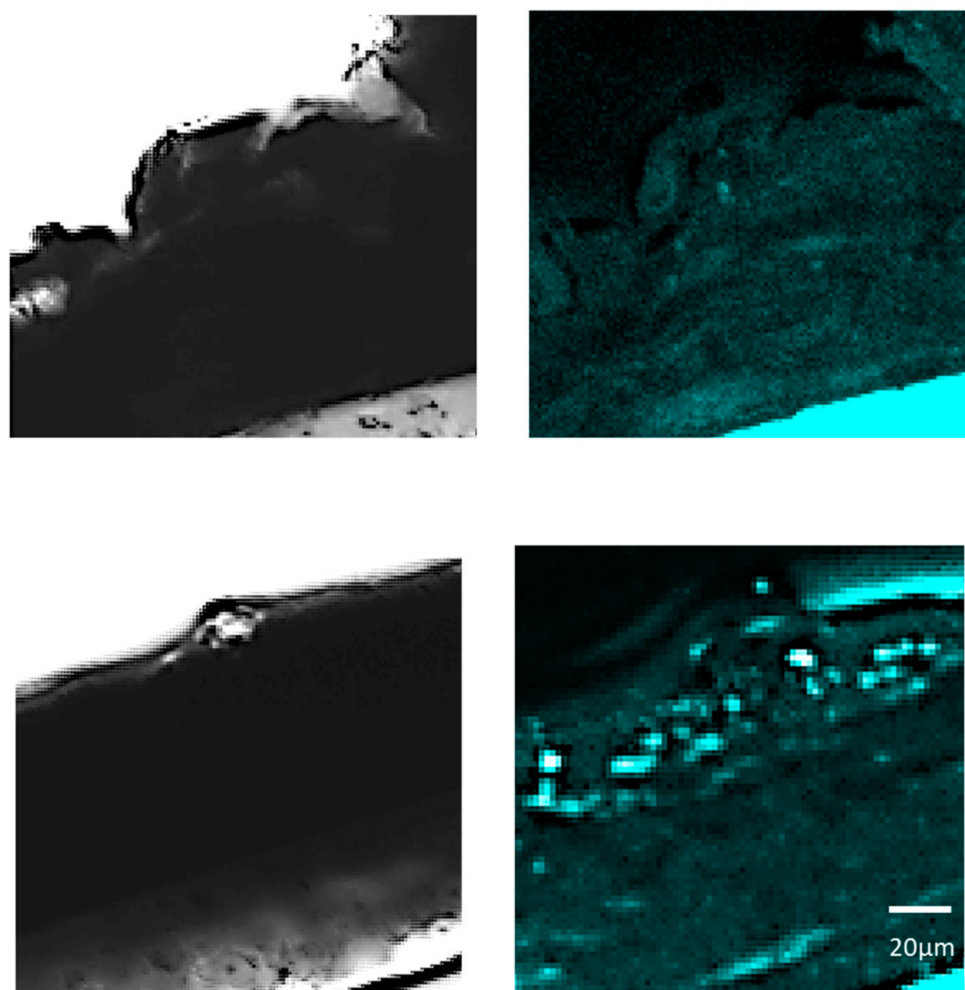


**Figure 4.** Fluorescence staining for CASP14 activity in the 3D epidermis models with topically applied LMHA or solvent (control). (**top**) Solvent-applied 3D epidermis model (control) (**left**: bright field, **right**: fluorescence), (**bottom**) LMHA-applied 3D epidermis model (**left**: bright field, **right**: fluorescence).

#### *3.4. Staining for CAPN1 Activity in the 3D Epidermis Models*

Staining was performed using Suc-LLVY-pNA as a substrate in tissue sections applied with LMHA or solvent (control) in which an increase in immunoreactive FLG was observed. FastBlue was used as the staining reagent, and the images were observed at 359/461 nm using an inverted confocal laser scanning microscope. In the 3D epidermis model with LMHA applied topically, slightly more fluorescence was observed from the stratum corneum to the stratum granulosum than in the control (Figure 5).

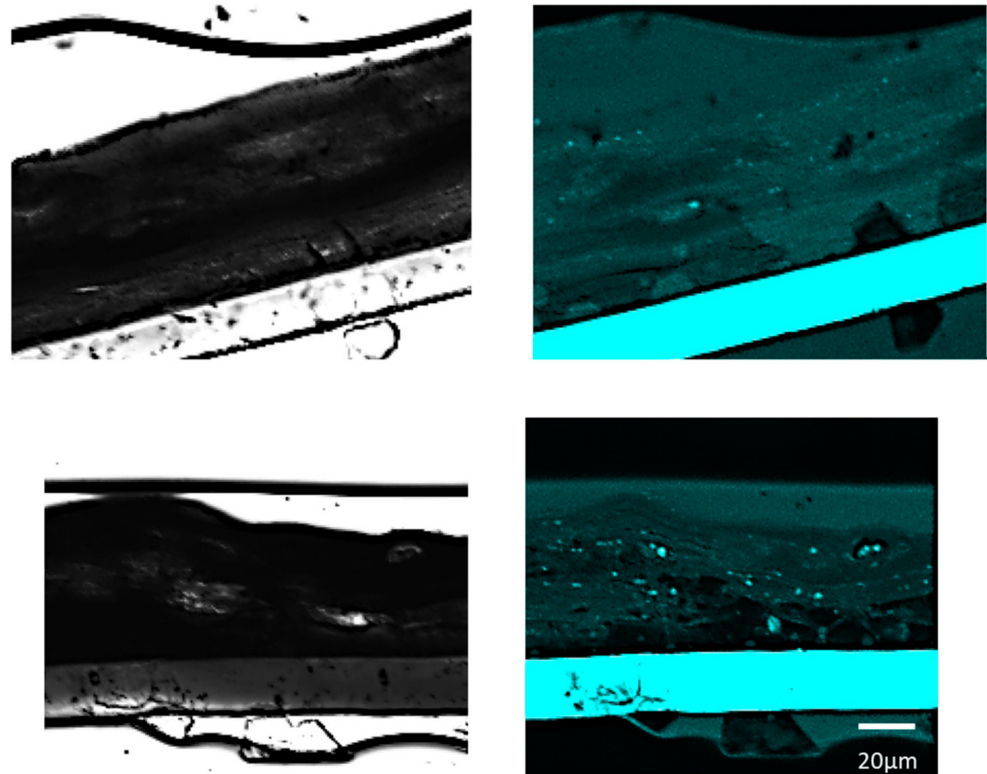


**Figure 5.** Fluorescence staining for CAPN1 activity in the 3D epidermis model with topically applied LMHA or solvent (control). (**top**) Solvent-applied 3D epidermis model (control) (**left**: bright field, **right**: fluorescence), (**bottom**) LMHA-applied 3D epidermis model (**left**: bright field, **right**: fluorescence).

### 3.5. Measurement of BLMH Activity Using Cultured Human Epidermal Keratinocytes

Since there was no substrate to which para-nitroanilide binds and FastBlue staining could not be performed on tissue sections, BLMH activity was measured using extracts of cultured human epidermal keratinocytes. The enzyme activity was calculated as the change in fluorescence intensity (0 min to 120 min)/protein amount. The results are shown in Figure 6. BLMH was significantly greater in the cultured human epidermal keratinocytes with LMHA than in the cultured human epidermal keratinocytes applied with solvent (control).

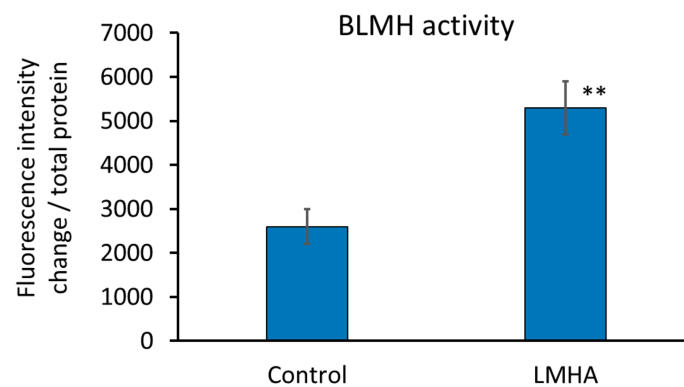
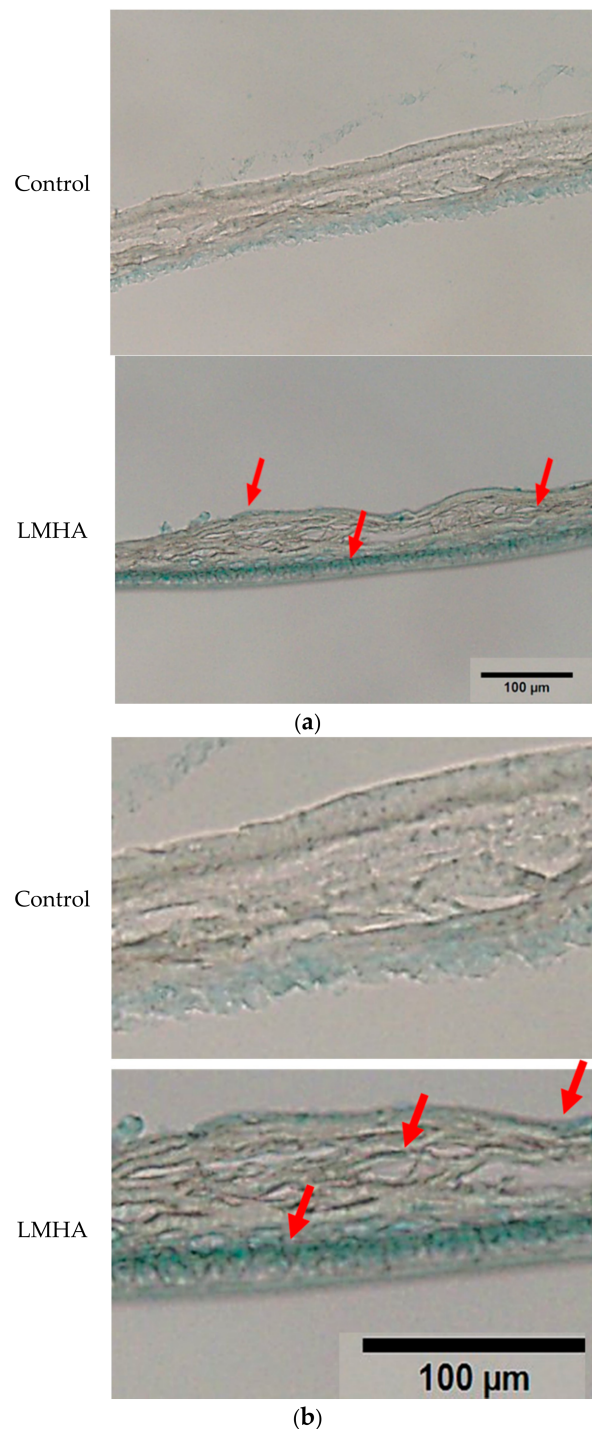


**Figure 6.** Effect of LMHA on BLMH activity in cultured human epidermal keratinocytes.  $n = 3$ , mean  $\pm$  standard deviation, \*\*  $p < 0.01$  vs. control.

### 3.6. Hyaluronan Staining of the 3D Epidermis Models

Tissue sections of the 3D epidermis models cultured with topical application of LMHA, or solvent (control) were stained with Alcian blue to determine the localization of hyaluro-

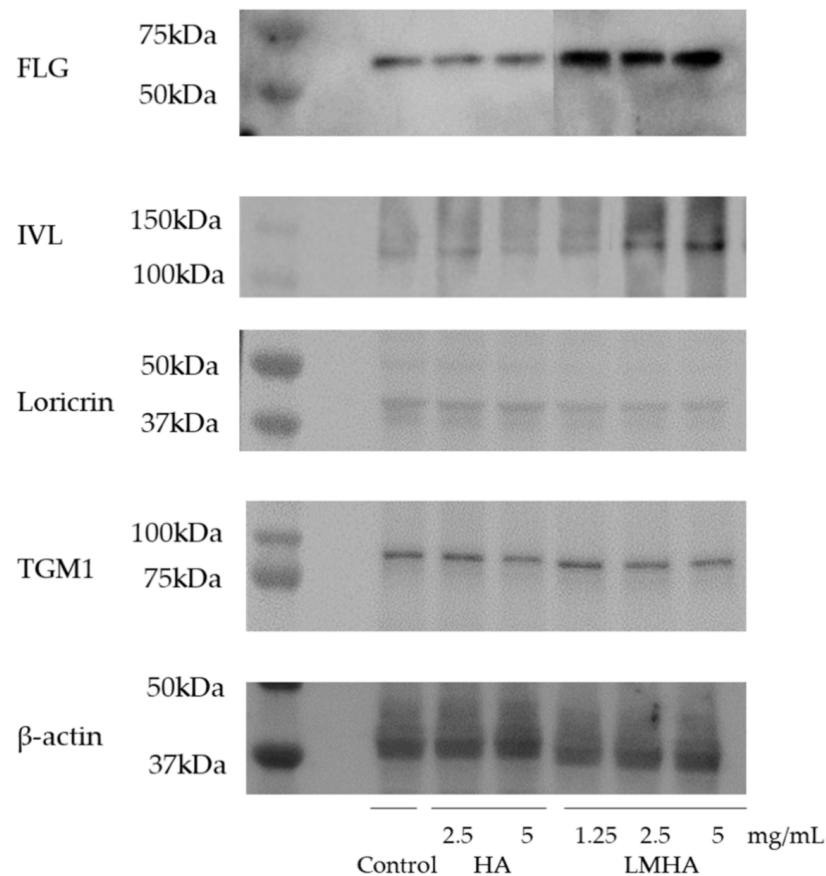
nan. Figure 7 shows the hyaluronan staining of an LMHA-applied 3D epidermis model (Figure 7b is an enlarged image of Figure 7a). In the LMHA-applied epidermis model, blue staining was observed in the granular layer and intense blue staining in the basal layer. Less staining was observed in the control-applied 3D epidermis model.



**Figure 7.** (a) Effects of topical application of LMHA on hyaluronan (Alcian blue staining) in the 3D epidermis model. The red arrows indicate the main areas where hyaluronan staining was observed. (b) Enlarged image of the effect of topical application of LMHA on hyaluronan (Alcian blue staining) in the 3D epidermis model. The red arrows indicate the main areas where hyaluronan staining was observed.

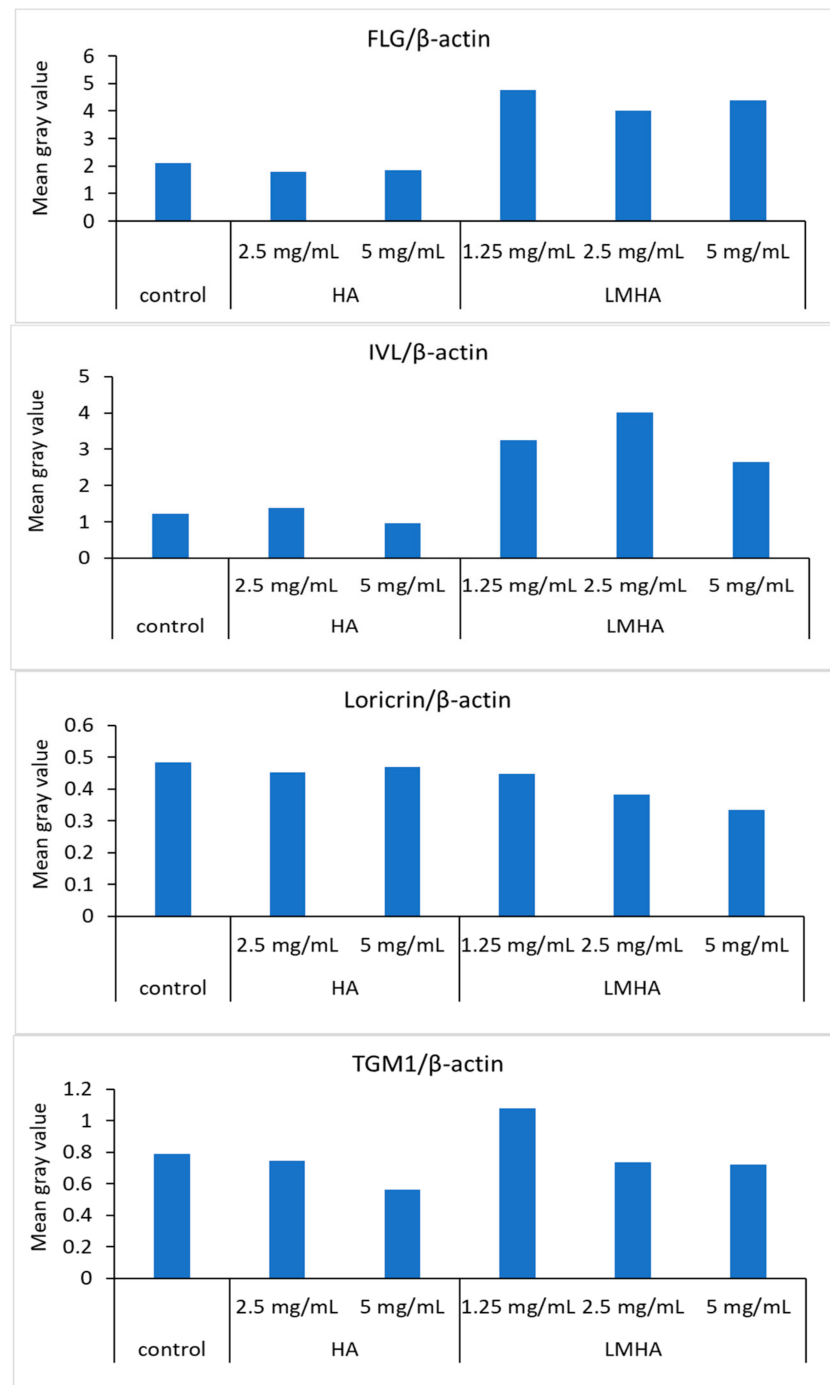
### 3.7. Western Blotting of Proteins Extracted from the 3D Epidermis Models with Topically Applied HA or LMHA

Figure 8 shows Western blotting results for FLG and for the differentiation markers IVL, loricrin, and TGM1, and  $\beta$ -actin from left to right as follows: control; 2.5 mg/mL HA; 5 mg/mL HA; 1.25 mg/mL LMHA; 2.5 mg/mL LMHA; and 5 mg/mL LMHA. Figure 9 shows the results of Western blotting of FLG, IVL, loricrin, and TGM1 proteins by image analysis. FLG protein and IVL protein, a marker of the granular layer, of 1.25 mg/mL, 2.5 mg/mL, and 5 mg/mL concentrations were significantly higher in the LMHA-applied model than in the solvent (control)- or HA-applied model at all concentrations. There was no significant difference in the amount of loricrin protein, which is expressed very late in epidermal differentiation, and TGM1 protein between the models applied with all concentrations of HA or LMHA and those applied with solvent (control).



**Figure 8.** Effects of topical application of HA and LMHA on FLG, IVL, loricrin, TGM1, and  $\beta$ -actin in the 3D epidermis model.





**Figure 9.** The results of Western blotting of HA and LMHA for FLG/ $\beta$ -actin, IVL/ $\beta$ -actin, loricrin/ $\beta$ -actin, and TGM1/ $\beta$ -actin by image analysis.

#### 4. Discussion

In the experiments using the 3D epidermis models, proFLG and IVL mRNA levels were increased by the topical application of LMHA. Western blotting showed that FLG and IVL were increased by LMHA. The cells of the stratum spinosum differentiate into the stratum granulosum and eventually into the stratum corneum. The stratum corneum forms CE consisting of proteins such as IVL and loricrin, which is responsible for the barrier function of the skin. The stratum granulosum expresses IVL and TGase. Loricrin, also a CE protein, is expressed and is confined to the granular layers of normal human epidermis. The expression of loricrin in human skin did not change after barrier disruption, but the expression of IVL, which was restricted to the granular layer and upper spinous layer in

normal human skin, was reported to show extension to the lower spinous layer 24 h after acetone treatment [25]. This suggests that the application of LMHA induces the IVL of granular and upper spinous layers, resulting in promoting differentiation.

Furthermore, immunofluorescence staining showed that topical application of LMHA increased the fluorescence intensity and the area of FLG protein in the 3D epidermis model. In the control 3D epidermis model, nuclear staining was observed near the stratum corneum, suggesting the occurrence of incomplete keratinization. Incomplete keratinization occurs when the rapid formation of keratinocytes does not allow denucleation to occur in time and the nuclei remain. This may be accompanied by a decrease in the granular layer. As the stratum corneum and granular layer decrease, FLG also decreases, resulting in a decrease in the fluorescence intensity and the area of FLG protein in the control 3D epidermis model.

FLG degradation is initiated by partial proteolysis by one or more unknown proteases deep in the stratum corneum. Further, cleavage by CASP14 efficiently degrades these fragments to free amino acids, which contribute to the production of NMF [26]. The proteolytic activation of CASP14 is associated with stratum corneum formation, implicating CASP14 in terminal keratinocyte differentiation and cornification [27,28]. When LMHA was applied topically to the 3D epidermis model, the mRNA level of CASP14 was increased, and the activity of CASP14 was increased in the stratum granulosum and stratum corneum. Increased mRNA for KLK7, which is involved in the maturation of CASP14 [8], supported that LMHA increased the activity of CASP14 by promoting the final differentiation of the epidermis. CAPN1 is also involved in this process; topical application of LMHA to the 3D epidermis model enhanced CAPN1 activity despite no change in CAPN1 mRNA levels; CAPN activity requires calcium ions [10], and the enhanced differentiation resulted in increased CAPN1 activity in the stratum granulosum and stratum corneum. The increase in calcium ions may have contributed to the increased activity of CAPN1. In addition, the mRNA level and activity of BLMH, which is believed to be involved in the breakdown of deiminated FLG into amino acids [4], was found to be significantly increased by LMHA in the cultured cell system. However, the localization of BLMH in the 3D epidermis model and whether its activity is increased by topical application of LMHA have not been investigated in this study, so it is necessary to investigate the activity of BLMH by staining using the 3D epidermis model in the future.

In the epidermal model with topically applied LMHA, Alcian blue staining showed localized hyaluronan near the stratum corneum. Blue staining was also seen in the stratum granulosum, and intense blue staining was seen in the basal layer of the epidermis. Under the conditions of the present study, Alcian blue stains mucopolysaccharides, but the blue staining observed in the basal layer of the epidermis may be due to the induction of mucopolysaccharides by topical application of LMHA.

These results suggest that HA of molecular weights of 10 kDa or less can penetrate deeper into the stratum corneum, affecting FLG-degrading enzymes in the stratum granulosum and mucopolysaccharides in the basal layer of epidermis.

## 5. Conclusions

LMHA increased the mRNA levels and activity of FLG and its degrading enzyme, CASP14, in the 3D epidermis models, and increased the activity of BLMH in the cultured keratinocytes. The increase in FLG protein was also confirmed by immunofluorescence and Western blotting, suggesting that topical application of LMHA to the skin can promote the biosynthesis of proFLG and upregulate FLG-degrading enzymes in human epidermis. In addition, topical application of LMHA was found to induce the production or accumulation of mucopolysaccharides in the basal layer of the epidermis. These results suggest that topical application of LMHA can promote the moisturizing effect by acting directly on the stratum corneum and indirectly from the stratum granulosum to the basal layer of the epidermis.

**Author Contributions:** M.H. and K.M. performed the experiments. K.M. designed the study and performed the data analysis. M.H. and K.M. interpreted the data and drafted the manuscript. K.M. supervised the study and critically revised the manuscript. All authors read and approved the final manuscript.

**Funding:** This research received no external funding.

**Institutional Review Board Statement:** Not applicable.

**Informed Consent Statement:** Not applicable.

**Data Availability Statement:** Not applicable.

**Conflicts of Interest:** The authors declare no conflict of interest.

## References

1. Pendaries, V.; Malaisse, J.; Pellerin, L.; Le Lamer, M.; Nachat, R.; Kezic, S.; Schmitt, A.M.; Paul, C.; Poumay, Y.; Serre, G.; et al. Knockdown of filaggrin in a three-dimensional reconstructed human epidermis impairs keratinocyte differentiation. *J. Investig. Dermatol.* **2014**, *134*, 2938–2946. [[CrossRef](#)]
2. Sakabe, J.; Yamamoto, M.; Hirakawa, S.; Motoyama, A.; Ohta, I.; Tatsuno, K.; Ito, T.; Kabashima, K.; Hibino, T.; Tokura, Y. Kallikrein-related peptidase 5 functions in proteolytic processing of profilaggrin in cultured human keratinocytes. *J. Biol. Chem.* **2013**, *288*, 17179–17189. [[CrossRef](#)]
3. Hsu, C.Y.; Henry, J.; Raymond, A.A.; Méchin, M.C.; Pendaries, V.; Nassar, D.; Hansmann, B.; Balica, S.; Burlet-Schiltz, O.; Schmitt, A.M.; et al. Deimination of human filaggrin-2 promotes its proteolysis by calpain 1. *J. Biol. Chem.* **2011**, *286*, 23222–23233. [[CrossRef](#)] [[PubMed](#)]
4. Kamata, Y.; Taniguchi, A.; Yamamoto, M.; Nomura, J.; Ishihara, K.; Takahara, H.; Hibino, T.; Takeda, A. Neutral cysteine protease bleomycin hydrolase is essential for the breakdown of deiminated filaggrin into amino acids. *J. Biol. Chem.* **2009**, *284*, 12829–12836. [[CrossRef](#)]
5. Yamamoto, M.; Makino, T.; Motoyama, A.; Miyai, M.; Tsuboi, R.; Hibino, T. Multiple pathways are involved in DNA degradation during keratinocyte terminal differentiation. *Cell Death Dis.* **2014**, *5*, 1181–1194. [[CrossRef](#)] [[PubMed](#)]
6. Palmer, C.N.; Irvine, A.D.; Terron-Kwiatkowski, A.; Zhao, Y.; Liao, H.; Lee, S.P.; Goudie, D.R.; Sandilands, A.; Campbell, L.E.; Smith, F.J.; et al. Common loss-of-function variants of the epidermis barrier protein filaggrin are a major predisposing factor for atopic dermatitis. *Nat. Genet.* **2006**, *38*, 441–446. [[CrossRef](#)]
7. Marenholz, I.; Nickel, R.; Rüschenhoff, F.; Schulz, F.; Esparza-Gordillo, J.; Kerscher, T.; Grüber, C.; Lau, S.; Worm, M.; Keil, T.; et al. Filaggrin loss-of-function mutations predispose to phenotypes involved in the atopic march. *J. Allergy Clin. Immunol.* **2006**, *118*, 866–871. [[CrossRef](#)]
8. Yamamoto, M.; Miyai, M.; Matsumoto, Y.; Tsuboi, R.; Hibino, T. Kallikrein-related peptidase-7 regulates caspase-14 maturation during keratinocyte terminal differentiation by generating an intermediate form. *J. Biol. Chem.* **2012**, *287*, 32825–32834. [[CrossRef](#)]
9. Jung, M.; Choi, J.; Lee, S.A.; Kim, H.; Hwang, J.; Choi, E.H. Pyrrolidone carboxylic acid levels or caspase-14 expression in the corneocytes of lesional skin correlates with clinical severity, skin barrier function and lesional inflammation in atopic dermatitis. *J. Dermatol. Sci.* **2014**, *76*, 231–239. [[CrossRef](#)] [[PubMed](#)]
10. Suzuki, K. Nomenclature of calcium dependent proteinase. *Biomed. Biochim. Acta* **1991**, *50*, 483–484. [[PubMed](#)]
11. Kamata, Y.; Yamamoto, M.; Kawakami, F.; Tsuboi, R.; Takeda, A.; Ishihara, K.; Hibino, T. Bleomycin hydrolase is regulated biphasically in a differentiation and cytokine-dependent manner. *J. Biol. Chem.* **2011**, *286*, 8204–8212. [[CrossRef](#)]
12. Komatsu, N.; Saijoh, K.; Toyama, T.; Ohka, R.; Otsuki, N.; Hussack, G.; Takehara, K.; Diamandis, E.P. Multiple tissue kallikrein mRNA and protein expression in normal skin and skin diseases. *Br. J. Dermatol.* **2005**, *153*, 274–281. [[CrossRef](#)]
13. Hansson, L.; Strömquist, M.; Bäckman, A.; Wallbrandt, P.; Carlstein, A.; Egelrud, T. Cloning, expression, and characterization of stratum corneum chymotryptic enzyme. A skin-specific human serine proteinase. *J. Biol. Chem.* **1994**, *269*, 19420–19426. [[CrossRef](#)]
14. Ekholm, I.E.; Brattsand, M.; Egelrud, T. Stratum corneum tryptic enzyme in normal epidermis: A missing link in the desquamation process? *J. Investig. Dermatol.* **2000**, *114*, 56–63. [[CrossRef](#)] [[PubMed](#)]
15. Yamasaki, K.; Schaubert, J.; Coda, A.; Lin, H.; Dorschner, R.A.; Schechter, N.M.; Bonnart, C.; Descargues, P.; Hovnanian, A.; Gallo, R.L. Kallikrein-mediated proteolysis regulates the antimicrobial effects of cathelicidins in skin. *FASEB J.* **2006**, *20*, 2068–2080. [[CrossRef](#)]
16. Caubet, C.; Jonca, N.; Brattsand, M.; Guerrin, M.; Bernard, D.; Schmidt, R.; Egelrud, T.; Simon, M.; Serre, G. Degradation of corneodesmosome proteins by two serine proteases of the kallikrein family, SCTE/KLK5/hK5 and SCCE/KLK7/hK7. *J. Investig. Dermatol.* **2004**, *122*, 1235–1244. [[CrossRef](#)] [[PubMed](#)]
17. Ovaere, P.; Lippens, S.; Vandenabeele, P.; Declercq, W. The emerging roles of serine protease cascades in the epidermis. *Trends Biochem. Sci.* **2009**, *34*, 453–463. [[CrossRef](#)]
18. Maytin, E.V.; Chung, H.H.; Seetharaman, V.M. Hyaluronan participates in the epidermis response to disruption of the permeability barrier in vivo. *Am. J. Pathol.* **2004**, *165*, 1331–1341. [[CrossRef](#)]

19. Kawada, C.; Yoshida, T.; Yoshida, H.; Matsuoka, R.; Sakamoto, W.; Odanaka, W.; Sato, T.; Yamasaki, T.; Kanemitsu, T.; Masuda, Y.; et al. Ingested hyaluronan moisturizes dry skin. *Nutr. J.* **2014**, *13*, 70–78. [[CrossRef](#)] [[PubMed](#)]
20. Essendoubi, M.; Gobinet, C.; Reynaud, R.; Angiboust, J.F.; Manfait, M.; Piot, O. Human skin penetration of hyaluronic acid of different molecular weights as probed by Raman spectroscopy. *Skin Res. Technol.* **2016**, *22*, 55–62. [[CrossRef](#)] [[PubMed](#)]
21. Farwick, M.; Gauglitz, G.; Pavicic, T.; Köhler, T.; Wegmann, M.; Schwach-Abdellaoui, K.; Malle, B.; Tarabin, V.; Schmitz, G.; Korting, H.C. Fifty-kDa hyaluronic acid upregulates some epidermal genes without changing TNF- $\alpha$  expression in reconstituted epidermis. *Skin Pharmacol. Physiol.* **2011**, *24*, 210–217. [[CrossRef](#)]
22. Radrezza, S.; Aiello, G.; Baron, G.; Aldini, G.; Carini, M.; D’Amato, A. Integratomics of human dermal fibroblasts treated with low molecular weight hyaluronic acid. *Molecules* **2021**, *26*, 5096. [[CrossRef](#)] [[PubMed](#)]
23. Sugiura, K.; Muro, Y.; Futamura, K.; Matsumoto, K.; Hashimoto, N.; Nishizawa, Y.; Nagasaka, T.; Saito, H.; Tomita, Y.; Usukura, J. The unfolded protein response is activated in differentiating epidermal keratinocytes. *J. Investig. Dermatol.* **2009**, *129*, 2126–2135. [[CrossRef](#)]
24. Morimoto, H.; Gu, L.; Zeng, L.; Maeda, K. Amino carbonylation of epidermal basement membrane inhibits epidermal cell function and is suppressed by methylparaben. *Cosmetics* **2017**, *4*, 38. [[CrossRef](#)]
25. Ekanayake-Mudiyanselage, S.; Aschauer, H.; Schmook, F.P.; Jensen, J.M.; Meingassner, J.G.; Proksch, E. Expression of epidermal keratins and the cornified envelope protein involucrin is influenced by permeability barrier disruption. *J. Investig. Dermatol.* **1998**, *111*, 517–523. [[CrossRef](#)] [[PubMed](#)]
26. Hoste, E.; Kemperman, P.M.; Devos, M.; Denecker, G.; Kežić, S.; Yau, N.; Gilbert, B.; Lippens, S.; de Groote, P.; Roelandt, R.; et al. Caspase-14 is required for filaggrin degradation to natural moisturizing factors in the skin. *J. Investig. Dermatol.* **2011**, *131*, 2233–2241. [[CrossRef](#)]
27. Eckhart, L.; Declercq, W.; Ban, J.; Rendl, M.; Lengauer, B.; Mayer, C.; Lippens, S.; Vandenabeele, P.; Tschachler, E. Terminal differentiation of human keratinocytes and stratum corneum formation is associated with caspase-14 activation. *J. Investig. Dermatol.* **2000**, *115*, 1148–1151. [[CrossRef](#)]
28. Denecker, G.; Hoste, E.; Gilbert, B.; Hochepped, T.; Ovaere, P.; Lippens, S.; Van den Broecke, C.; Van Damme, P.; D’Herde, K.; Hachem, J.P.; et al. Caspase-14 protects against epidermal UVB photodamage and water loss. *Nat. Cell Biol.* **2007**, *9*, 666–674. [[CrossRef](#)] [[PubMed](#)]